Synthesis of porous LaNiO$_3$ thin film by chemical solution deposition for enhanced oxygen evolution reaction

Min Zhu[a*], Zongqiang Sheng[a], Juan Gao[a], Yang Li[a], Chao Zhang[b*],

Xuebin Zhu[c]

Experimental section

Synthesis of LNO thin films

The LaNiO$_3$ thin films were deposited on Pt/Ti/SiO$_2$/Si substrates through chemical solution deposition method. The starting materials were Lanthanum (III) nitrate [La(NO$_3$)$_3$·6H$_2$O] and nickel (II) acetate [Ni(CH$_3$COO)$_2$·4H$_2$O], and 2-methoxyethanol was used as the solvent. Firstly La(NO$_3$)$_3$·6H$_2$O and Ni(CH$_3$COO)$_2$·4H$_2$O were added in 2-methoxyethanol respectively, and then they were stirred at a temperature of 70 °C for 10 min. Secondly two dissolved solutions were mixed up at this temperature and stirred for 5 hours at room temperature. The concentration of obtained precursor solution was adjusted to 0.2 mol/L. In the process of stirring, the F-127 copolymer was added into the precursor solution to introduce pores. The thin film was spin coated on Pt/Ti/SiO$_2$/Si substrate with a rotation speed of 5000 rpm for 20s, and baked at 400 °C for 5 min in air in order to volatilize the organic matter. Then the baked film was annealing at 700 °C for 20 min in air. To increase the film thickness, the spin-coating, baking and annealing processes were repeated for several times. For comparison, the normal LNO thin film was prepared by the similar method to the porous LNO film except the addition of F-127.

Materials characterization

The structural properties of thin films are characterized by using a Philips X'Pert PRO x-ray diffractometer with Cu Kα radiation. Field emission scanning electron microscopy (FE-SEM, Gemini SEM 500) and transmission electron microscopy (TEM, JEM-2100) were conducted to study the morphology and structure of the thin films. X-ray photoelectron spectroscopy (XPS) with monochromatic Al Kα (hv=1486.6 eV) was carried to evaluate the chemical states of the samples. All binding energies were referenced to the C 1s peak at 284.8 eV.

Electrochemical measurements

All of the electrochemical measurements were performed on CHI 660E electrochemical workstation at ambient temperature and pressure. A conventional three-electrode system, which contained a platinum wire used as counter electrode and a Hg/HgO electrode (1 M KOH) as reference electrode, was applied to conducted the electrochemical test. And the sample of porous LNO thin films on the Pt/Ti/SiO$_2$/Si substrate was directly used as the working electrodes. For the preparation of RuO$_2$ electrodes, 6 mg of catalysts were dispersed in 880 μL ethanol and 20 μL nafion (5 wt.%) mixed

solutions. And the above mixed solution was sonicated for 30 min to form a uniform ink. Then 150 μL catalysts ink was dropped onto a piece of carbon paper (1×1 cm^2, catalysts loading 1 mg cm^{-2}) and dried at room temperature. O$_2$-saturated 1 M KOH solution was used as the electrolyte for the electrochemical measurements. All of the linear sweep voltammetry (LSV) polarization curves were corrected with iR compensation.
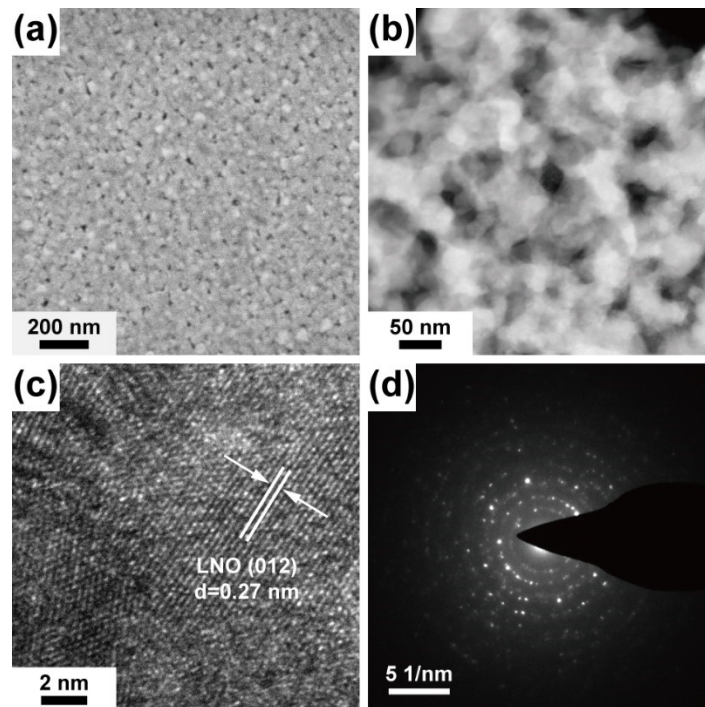
Figure S1. (a) The SEM image, (b) HADDF-STEM image, (c) HRTEM image and (d) corresponding SAED pattern of LNO film.
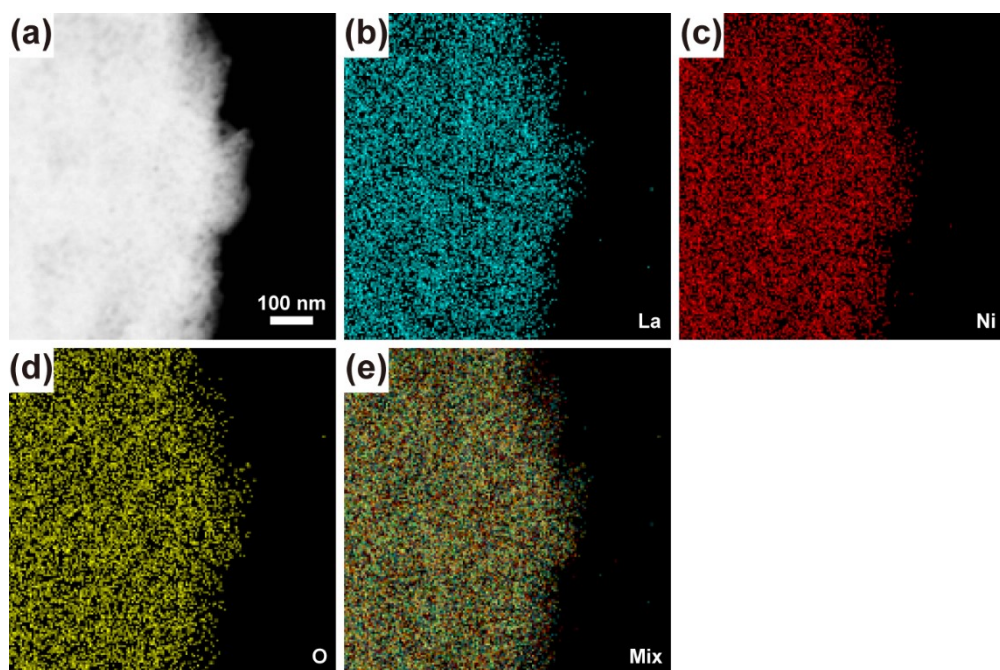
Figure S2. (a) HADDF-STEM image and (b-e) the corresponding elemental mapping images of LNO film.
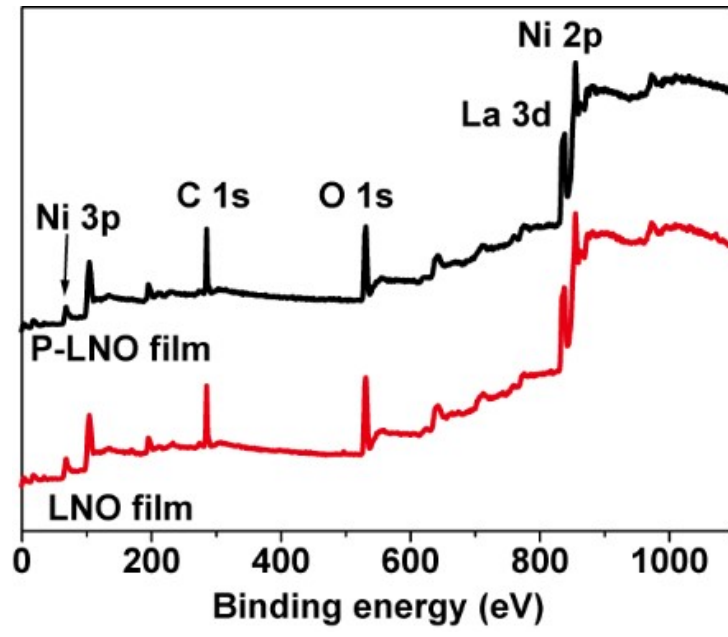
Figure S3. The survey XPS spectrum of P-LNO film and LNO film.
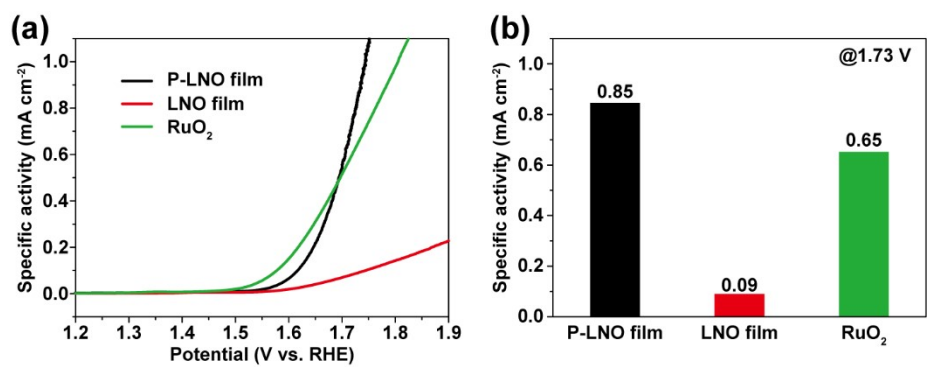
Figure S4. (a) The LSV curves normalized by ECSA derived from C_{dl} and (b) the specific activity at 1.73 V of P-LNO film, LNO film and RuO_2.
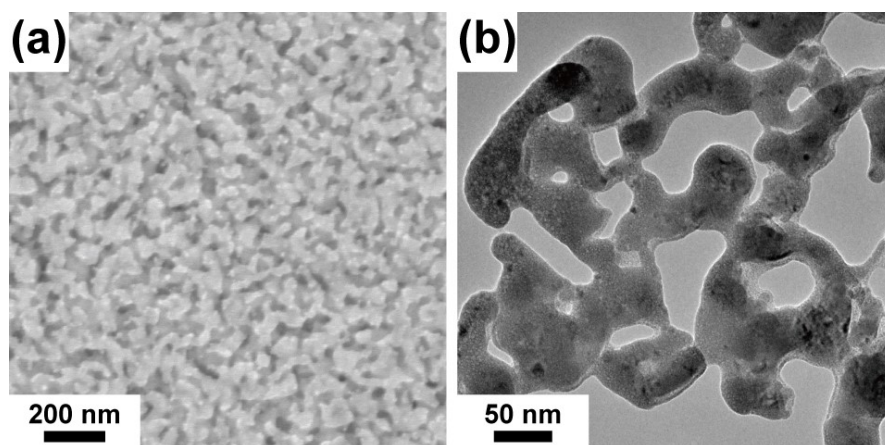
Figure S5. (a) The SEM image and (b) TEM image of P-LNO film after OER stability test.
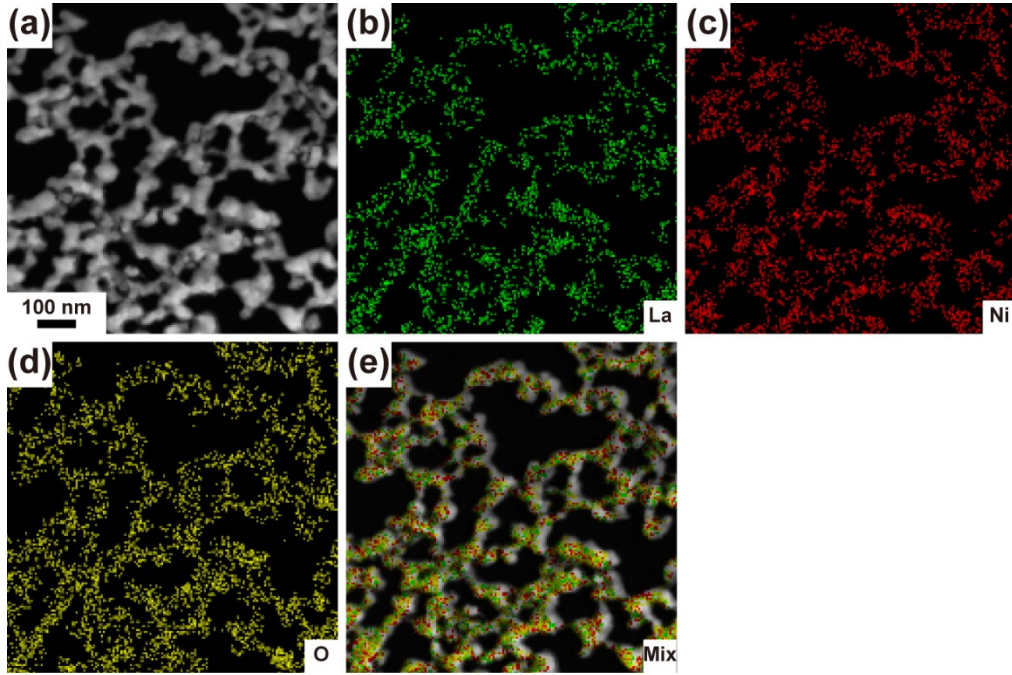
Figure S6. (a) HADDF-STEM image and (b-e) the corresponding elemental mapping images of P-LNO film after stability test.
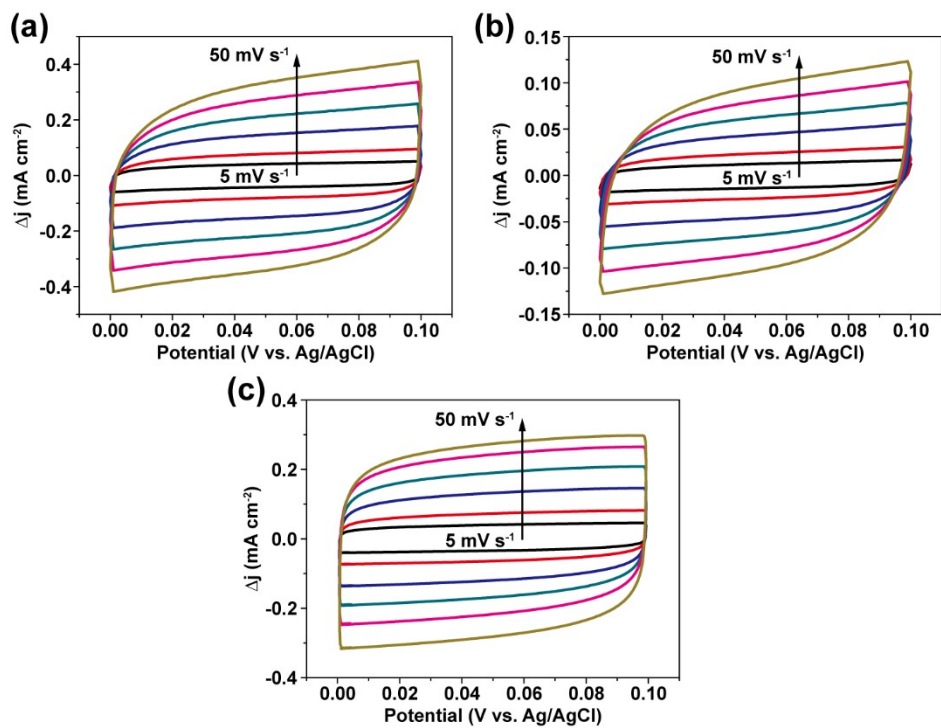
Figure S7. The CV curves of (a) P-LNO film, (b) LNO film and (c) RuO$_2$ under different scan rates in the region of 0~0.1 V vs. Ag/AgCl.

Table S1. The comparison of the OER performance for P-LNO film, LNO film and RuO_2 in 1 M KOH.

	Overpotential @ 10 mA cm^{-2} (mV)	Current density @ 450 mV (mA cm^{-2})	Tafel slope (mV dec^{-1})
P-LNO film	367	64.7	95.2
LNO film	350	7.6	127.5
RuO_2	478	41.3	124.9

Table S2. Comparison of OER activities for porous $LaNiO_3$ with recent reported perovskite-based OER catalysts.

Catalysts	$\eta_{10\,mA\,cm^{-2}}$ (mV)	Ref.
porous $LaNiO_3$	367	This work
$LaCoO_3$	470	Chem, 2017, 3, 812
$La_{0.9}Sn_{0.1}NiO_{3-\delta}$	318	J. Mater. Chem. A, 2022, 10, 1336
$LaFeO_3$	420	Adv. Mater. Interfaces, 2019, 6, 1801317
$La_{0.96}Ce_{0.04}CoO_3$	380	Nanoscale, 2021, 13, 9952
$Sr_{0.95}Ce_{0.05}Fe_{0.9}Ni_{0.1}O_{3-\delta}$	340	Adv. Funct. Mater., 2022, 32, 2111091
$La_{0.6}Sr_{0.4}Co_{0.8}Fe_{0.2}O_3$	353	ACS Appl. Mater. Interfaces 2019, 11, 47858.
$LaCo_{0.75}Fe_{0.25}O_3$	310	Small, 2022, 18, 2201131
$La_{0.95}Fe_{0.8}Co_{0.2}O_3$	377	J. Alloys Compd., 2021, 854, 157154
$LaFe_{0.25}Ni_{0.75}O_3$	287	ACS Appl. Mater. Interfaces, 2020, 12, 41259
$Sm_{0.5}Sr_{0.5}Fe_{0.8}Co_{0.2}O_{3-\delta}$	316	Sustain. Energ. Fuel, 2021, 5, 4858
$SrCo_{0.9}Fe_{0.1}O_{3-\delta}$	370	SusMat., 2022, 2, 445
$La_{0.5}Pr_{0.5}CoO_3$	312	ACS Appl. Energy Mater. 2021, 4, 9057
$Bi_{0.15}Sr_{0.85}Co_{0.8}Fe_{0.2}O_{3-\delta}$	354	J. Mater. Sci. Technol., 2022, 108, 158